

# Polymeric Membranes of Chitosan/Aloe Vera Gel Fabrication With Enhanced Swelling and Antimicrobial Properties for Biomedical Applications

Dose-Response:  
An International Journal  
April-June 2023:1–12  
© The Author(s) 2023  
Article reuse guidelines:  
[sagepub.com/journals-permissions](https://sagepub.com/journals-permissions)  
DOI: 10.1177/15593258231169387  
[journals.sagepub.com/home/dos](https://journals.sagepub.com/home/dos)  


Dure N. Iqbal<sup>1</sup>, Atira Munir<sup>1</sup>, Mazhar Abbas<sup>2</sup>, Arif Nazir<sup>1</sup> , Zahid Ali<sup>1,3</sup>, Samar Z. Alshawwa<sup>4</sup> , Munawar Iqbal<sup>1,5</sup> , and Naveed Ahmad<sup>5</sup>

## Abstract

Since ancient times, medicinal plants have been used as traditional medicine to treat a variety of ailments. Aloe vera (AV) gel's therapeutic potential is one of the most effective approach in the fabrication of functional materials. The current study aimed to prepare the AV and chitosan (CS) membranes using various cross-linkers that were characterized using X-ray diffraction (XRD), scanning electron microscopy (SEM), Fourier transform-infrared (FT-IR) spectroscopy, thermal gravimetric analysis (TGA), and ultraviolet-visible (UV-Visible) techniques, as well as swelling ratio and antimicrobial studies. SEM analysis revealed that the membrane is porous, with interconnected pores. The inclusion of AV contents in the membrane improved thermal stability and crystallinity. The swelling ratio of the ACPG-3 membrane with a 2:1 CS to AV ratio was 366%. The membranes showed promising antimicrobial activity against *Escherichia coli*, *Staphylococcus aureus*, *Bacillus subtilis*, and *Pasteurella multocida* strains. The findings revealed that polymeric CS/AV membranes have effective potential for use in the biomedical field.

## Keywords

chitosan, aloe vera gel, polymeric membranes, antimicrobial activity, wound dressing

## Introduction

Wound healing is a complex and ongoing process in which injured tissues are repaired and an efficient system is required to improve the healing process. There are numerous ointments and bandages available for treatment. Commonly used synthetic polymeric bandages have poor healing efficacy for chronic wounds.<sup>1-3</sup> The significant limitations of skin injury treatment formulations such as gels and ointments include their inability to sustain the release of medicine for an extended period of time at wet injury sites due to their short-lived existence.<sup>4,5</sup> Furthermore, these dressings do not provide adequate moisture, pH, or gas exchange to injured skin. These conditions promote the growth of bacteria and the spread of infection which slows the healing process.<sup>6</sup> As a result, many efforts have been made to create high-quality wound dressing materials that are natural and biodegradable in order to speed up the healing process.<sup>7-10</sup> Recently, medicinal plants have

been used as a medicine substitute.<sup>11,12</sup> The phytochemicals derived from plants have medicinal properties that are used to treat a variety of infections. Over the past few years, aloe vera

- 
- <sup>1</sup> Department of Chemistry, The University of Lahore, Lahore, Pakistan  
<sup>2</sup> Department of Biochemistry, University of Veterinary and Animal Sciences, Lahore, Pakistan  
<sup>3</sup> State Key-Laboratory of Organic Inorganic-Composites, Beijing University of Chemical Technology, Beijing, China  
<sup>4</sup> Department of Pharmaceutical Sciences, College of Pharmacy, Princess Nourah bint Abdulrahman University, Riyadh, Saudi Arabia  
<sup>5</sup> Department of Chemistry, Division of Science and Technology, University of Education, Lahore, Pakistan

Received 10 November 2022; accepted 27 March 2023

### Corresponding Author:

Arif Nazir, Department of Chemistry, The University of Lahore, Lahore 53700, Pakistan.  
Email: [arif.nazir@chem.uol.edu.pk](mailto:arif.nazir@chem.uol.edu.pk)



Creative Commons Non Commercial CC BY-NC: This article is distributed under the terms of the Creative Commons Attribution-NonCommercial 4.0 License (<https://creativecommons.org/licenses/by-nc/4.0/>) which permits non-commercial use, reproduction and distribution of the work without further permission provided the original work is attributed as specified on the SAGE

and Open Access pages (<https://us.sagepub.com/en-us/nam/open-access-at-sage>).

has been the focus of extensive scientific research due to its therapeutic benefits.<sup>13,14</sup> It is known as “the healing and wonder plant.” Due to its anti-inflammatory, antibacterial, and wound-healing characteristics, aloe vera has long been used to treat digestive issues as well as skin injuries (burns, wounds, insect bites, and eczemas). The goal of research on this medicinal plant was to understand its mode of action and to pinpoint the chemicals responsible for these effects.<sup>7</sup> The active components of aloe vera gel are vitamins (A, B<sub>12</sub>, C, E, choline, and folic acid), enzymes (basic phosphatase, amylase, carboxypeptidase, bard kinase, catalase, lipase, cellulase, and peroxidase), minerals (copper, chromium, calcium, selenium, manganese, magnesium, zinc, sodium, and potassium),<sup>8-10</sup> carbohydrate (fructose, glucose, and glucomannan),<sup>11,12</sup> anthraquinones, folic acids (cholesterol,  $\beta$ -sitosterol, lupeol, and camp sterol), hormones (gibberellins and auxins), amino acids, salicylic acid, lignins, and saponins. The active ingredients that have received the greatest research are acemannan, aloe-emodin, aloin, aloes, and emodin.<sup>13</sup>

The majority of in vitro research on skin protection examined that how *Aloe vera* and its active ingredients aid in wound healing. The most popular cell lines are fibroblasts, primary normal human epidermal keratinocytes (HEKa), and immortalized human keratinocytes (HaCaT). These research studies have shown that aloe vera and its active ingredients (aloes, aloin, and emodin) exert their protective effects primarily through anti-inflammatory and antioxidant processes to safeguard the body.<sup>14-16</sup>

Additionally, chitosan, a bio-polymeric material, had been broadly utilized as a base substance for wound therapy due to its distinctive set of biological features, which include biocompatibility, biodegradability, and low toxicity. Chitosan also has mucoadhesive, hemostatic, and antibacterial characteristics and may speed up the healing of wounds.<sup>17-19</sup>

In order to create a new class of compounds known as biosynthetic polymeric blends or bio-artificial materials with better mechanical strength, thermal stability, and biocompatibility as compared to individual components that are likely to be administered for many medicinal purposes, the natural polymeric blends are combined with synthetic polymers because they exhibit poor mechanical efficacies. Bio-artificial mixing's goal is to create semi-synthetic blends with specific structural characteristics and tensile strengths depending on specified biopolymer and synthetic polymer attributes.<sup>20</sup> The polyvinyl alcohol (PVA) is a man-made, cost-effective, nontoxic, and water-miscible polymer. The film of PVA has superior quality and possesses good tensile strength and elastic nature with diverse implementations in various disciplines, such as artificial muscle, contact lenses, ignited wound bandages, and vocal band reformation.<sup>21,22</sup> The phenomenon of wound curing is very complex that can show several irregularities. So, the choice of proper wound bandage is very crucial to guide and enhance the curing action.<sup>23</sup>

Therefore, the objective of the present work is to develop a synergic relationship between chitosan and aloe vera gel to

design a polymeric blended bio-membrane through solution casting process that is likely to be utilized as an effective skin lesion bandage for providing a novel approach for wound therapy. The potentiality of various cross-linkers inclusion on physicochemical performance of AV/CS-based polymeric membranes was also assessed. The fabricated membranes were characterized by UV-visible, FT-IR, XRD, SEM, and TGA techniques. The antimicrobial activity and swelling ratio of AV/CS-based films were also investigated.

## Material and Methods

### Chemicals and Reagents

Chitosan has been obtained from GmbH Germany, CH<sub>3</sub>COOH, Tween 80, and polyvinyl alcohol from ICI American, Inc. Glycerol from Antares Chemical Pvt. Limited, India, and glutaraldehyde from Sigma-Aldrich, Germany. All the chemicals were of analytical grade and were used without further processing.

### Aloe Vera Gel Extraction

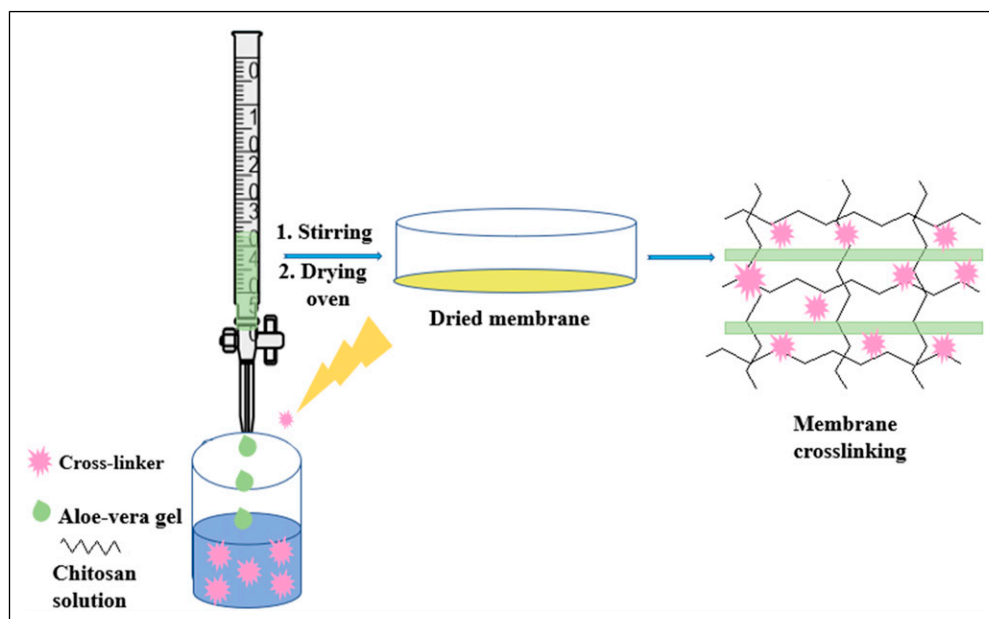
For the extraction of *Aloe vera* gel, 2 years old aloe vera plants are selected from the local garden of Lahore. The aloe vera leaves have been separated from the plant and cleaned with distilled H<sub>2</sub>O to eliminate dirt particles superficially. The dermis is removed with the help of a sharp knife. The specimens were washed vigorously with water to clean the surface. The AV gel is put in a blender for homogenization and subsequently filtered. The homogenized mixture is heated at 60°C for 30 min for stabilization.<sup>24,25</sup>

### Chitosan and Aloe vera Membranes Preparation

For ACPG membranes, 60% CS powder is solubilized gradually for 8 h in a 2% acetic acid solution. 20% PVA crystals are suspended in 30 mL distilled water at boiling temperature. Then, the solution of PVA and 10% glycerol (plasticizer) is added to this mixture, blended, and stirred for 5 h. After that, 10% AV gel is dispersed in 30 mL distilled water at 50°C for 1 h till complete dissolution and above suspension was added and mixed well. For fabrication of ACGG membranes, 20% AV are suspended in 100 mL distilled water at 75°C with continuous blending and stirring unless no crystal is left undissolved. 10% glutaraldehyde is mixed with 20 mL distilled water and added with constant stirring. Then this mixture is suspended to the CS solution, blended, and stirred till complete dissolution. For the synthesis of CAT membranes, 10% Tween 80 was added to CS and AV solution. Subsequently, the mixture is subjected to sonication to remove any entrapped air bubbles. After that, this mixture is casted in the petri plate and desiccated at 40°C in the drying oven for 24 h (Table 1, Figure 1). The membranes were neutralized by soaking in 4% NaOH/ethanol 1:1 for 15 min,

**Table I.** CS/AV Membranes Composition with Sample Code.

Sr NO	Sample Code	Chitosan (%)	Aloe vera (%)	PVA/Glutaraldehyde/Tween80 (%)
1	ACPG	70	0.0	20
2	ACPG-1	60	10	20
3	ACPG-2	50	20	20
4	ACPG-3	40	30	20
5	ACGG	70	0.0	10
6	ACGG-1	60	10	10
7	ACGG-2	50	20	10
8	ACGG-3	40	30	10
9	CAT	90	0.0	10
10	CAT-1	80	10	10
11	CAT-2	70	20	10
12	CAT-3	60	30	10

**Figure 1.** Schematic presentation for the preparation of AV-gel-based membrane.

followed by rinsing in ethanol and distilled water until pH 7 was obtained.

### Characterization of the Membranes

SEM investigation of fabricated films was employed with FEI-NOVA-450 Nano SEM (FE-SEM), USA. XRD analysis was studied by AXS-D8 advanced X-ray diffractometer (Bruker, USA), with a range from 0 to 80, 2 Theta. UV-visible analysis was performed by Cecil-Aquarius 7400 Ce, UK. FT-IR (Alpha II, Bruker, USA) is used to characterize functional groups at scanning range of 4000–625  $\text{cm}^{-1}$ . TGA-250 (Bruker, USA) at heating rate 10 $^{\circ}$ /min under nitrogen atmosphere was used to investigate thermal stabilization. Prepared hydrogels were

subjected to the subsequent method for swelling examination. The membrane of fixed mass was soaked in a beaker containing the distilled water at an ambient temperature. After a specific time, excessive solvent was discarded and weight of puffed membrane was computed. The membranes were immersed in the solvent again till it achieved equilibrium state. The swelling and equilibrium swelling was estimated using equations 1 and 2<sup>26</sup>

$$\text{Swelling} = \frac{W_S - W_D}{W_D} \quad [1]$$

$$\text{Equilibrium Swelling (\%)} = \frac{W_S - W_D}{W_S} \times 100 \quad [2]$$

## Antimicrobial Activity

**Bacterial Strains.** Following Gram-positive and Gram-negative bacterial strains,<sup>1</sup> *E. coli*,<sup>2</sup> *P. multocida*,<sup>3</sup> *S. aureus*,<sup>4</sup> and *B. subtilis* were used to study the antimicrobial activities of chitosan/AV-based polymeric membranes.

**Bacterial growth medium, cultures, and inoculum preparation.** Pure cultures were maintained on a nutrient agar medium in the slants. For the inoculum preparation, 1.3 g/100 mL of nutrient broth (Oxoid, UK) was suspended in distilled water, heated, mixed well, and distributed homogeneously and autoclaved. Pure (100  $\mu$ L) culture of a bacterial strain was mixed with the medium and placed for 24 h at 37°C in a shaker 120 r/min. All the inoculum was prepared by the same pattern and stored at 4°C. The inoculum with  $1 \times 10^8$  CFU/mL was used for further analysis.

**Antibacterial Assay.** Antimicrobial activity of chitosan/AV-based polymeric membranes was determined using disc diffusion method (CLSI, 2011). 2.8 g/100 mL of nutrient agar (Oxoid, UK) was suspended in distilled water, mixed well, and distributed homogeneously. The medium was sterilized by autoclaving at 121°C for 15 min. Before the medium was transferred to petri plates, inoculum (100  $\mu$ L/100 mL) was added to the medium and poured in sterilized petri plates. After this, different synthesized membranes and antibiotic discs (norfloxacin; 10  $\mu$ g, catalogue number CT0434 B) of size 5 mm were laid flat on the growth medium containing medium. The petri plates were then incubated at 37°C for 24 h for the growth of bacteria. The extracts having antibacterial activity, inhibited the bacterial growth and clear zones were formed. The zones of inhibition were measured in millimeters using a zone reader.<sup>27</sup>

## Results and Discussion

*Aloe vera*/chitosan-based membranes have been synthesized successfully by using different cross-linkers. *Aloe vera* enhances collagen production due to the interlinking of glucomannan with gibberellin (growth receptor) present in the fibroblast.<sup>28</sup> More amount of collagen III is produced and crosslinking degree of collagen is also enhanced.<sup>29</sup> All these factors facilitate skin lesion contraction and amplify the cracking power of resultant scar tissues to help wound healing.<sup>30</sup> Chitosan has been extensively employed in various medicinal applications owing to its distinctive features such as bio adsorbable, nonpoisonous, antimicrobial, and bio-acceptable. It is of great interest to use chitosan as a wound curing agent because it encourages hemostasis and tissue reformation. It has been used for the treatment of burns, ulcers, and wounds.<sup>31</sup>

### Functional Group Analysis of the Membrane

It is a way of chemical characterization for the functional class identification of polymeric, inorganic, and organic

substances.<sup>32</sup> The investigation of functional moieties in fabricated hydrogels based on AV and chitosan was examined by FTIR spectroscopy. The generating characteristic peaks and responses are presented in Figure 2. The spectra of all blended membranes specify the particular peaks of AV and chitosan which are directly related to the individual content ratios in the membrane. The N-H and C = O peaks which appear between 1645 and 1670  $\text{cm}^{-1}$  are occupied by a single peak at 1656  $\text{cm}^{-1}$  in ACGG-3, 1652  $\text{cm}^{-1}$  in ACGG-2, 1657  $\text{cm}^{-1}$  in ACPG-3, 1640  $\text{cm}^{-1}$  in ACPG-2, 1652  $\text{cm}^{-1}$  in CAT-3, and 1650  $\text{cm}^{-1}$  in CAT-2 which proposed certain interactions between AV and CS. Various researchers have manifested that chitosan makes a bond with selected anionic molecules like nucleic acid, proteins, and polysaccharides.<sup>33</sup> AV gel consists of complex dissolute of proteins and polysaccharides.<sup>34</sup> Distinct interactions like H-bonding can exist between AV gel and CS to describe the noticed bond shift.<sup>24</sup>

The IR spectra of ACGG-2 and ACGG-3 point out the existence of new bonds between AV, CS, and glutaraldehyde as the spectra exhibit characteristic peaks at a particular area. A wide peak at about 3400  $\text{cm}^{-1}$  is noticed, which is the stretching vibration mark for the O-H group. The bending vibration peak at 1330  $\text{cm}^{-1}$  for O-H of chitosan is reduced to the smallest which specifies the crosslinking with glutaraldehyde.<sup>35</sup> The IR spectra of ACPG-2 and ACPG-3 demonstrated a slight peak shift which stipulated fabrication of the membrane. It displays C-H *str* at 2860–2930  $\text{cm}^{-1}$ , and a wider peak at 3200–3400  $\text{cm}^{-1}$  is responsible for O-H *str*. An exact band at 1640  $\text{cm}^{-1}$  indicates N-H *ben*, C-H ring absorption at 950  $\text{cm}^{-1}$ , C-O-H *ben* at 1440–1450  $\text{cm}^{-1}$ , ether C-O absorption at 1150  $\text{cm}^{-1}$ , and a characteristic glycosidic bond absorption at 1040–1070  $\text{cm}^{-1}$  is observed.

The IR spectra of CAT-2 and CAT-3 manifest the synthesis of blend based on CS, AV, and TW. The characteristic broad peaks observed as O-H *str* at 3200–3400  $\text{cm}^{-1}$  corroborate that such groups are responsible for H-bond between individual components of blend. The interfacial intermolecular H-bond is further authenticated by the existence of very broad bands of O-H ranging between 3100 and 3600  $\text{cm}^{-1}$ .<sup>36</sup> A sharp peak originated at 1650  $\text{cm}^{-1}$  indicating N-H *ben*. A characteristic peak at 1430–1435  $\text{cm}^{-1}$  is responsible for C-O-H *ben*. An exact absorption peak at 1250  $\text{cm}^{-1}$  indicates a glucan unit. A small peak at 1155  $\text{cm}^{-1}$  of ether C-O is observed, 2 absorption peaks of glycosidic bonding occur at 1020  $\text{cm}^{-1}$  and 1070  $\text{cm}^{-1}$ , and CH ring absorption exists at 955  $\text{cm}^{-1}$  and 960  $\text{cm}^{-1}$  in CAT-3 and 2, respectively.

### UV-Vis Analysis

Light transmittance is an important characteristic for membranes during wound curing applications.<sup>37</sup> The spectra of ACPG-3 and ACPG-2 point out the typical absorbance peaks ranged between 315–517 nm and 310–511 nm (Figure 3). The absorbance peak at 420 nm was indicated for CS membranes cross-linked with tween 80.<sup>38</sup> The absorbance peak of CS with

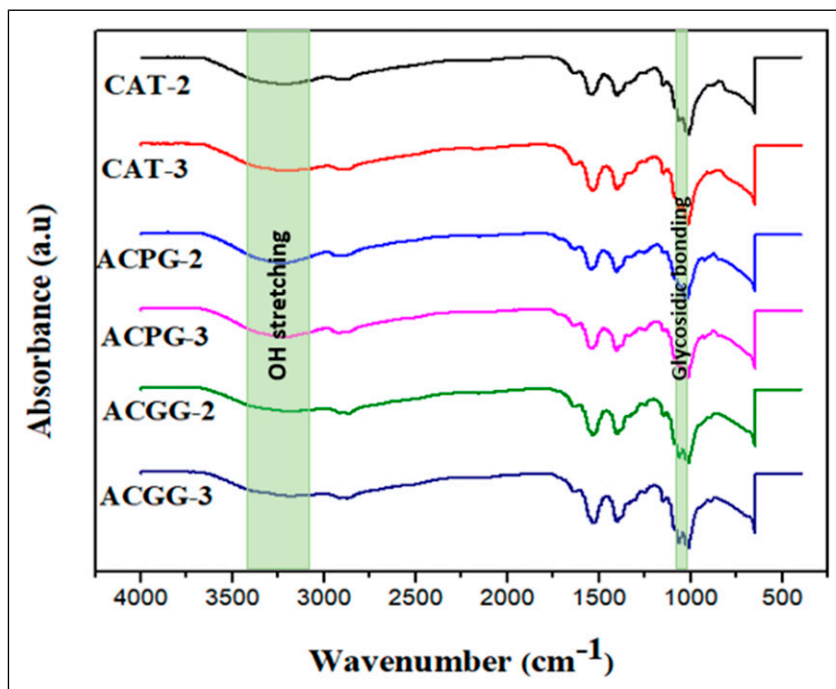


**Figure 2.** (a) FTIR analysis of ACGG 2-3, ACPG 2-3, and CAT 2-3 samples.

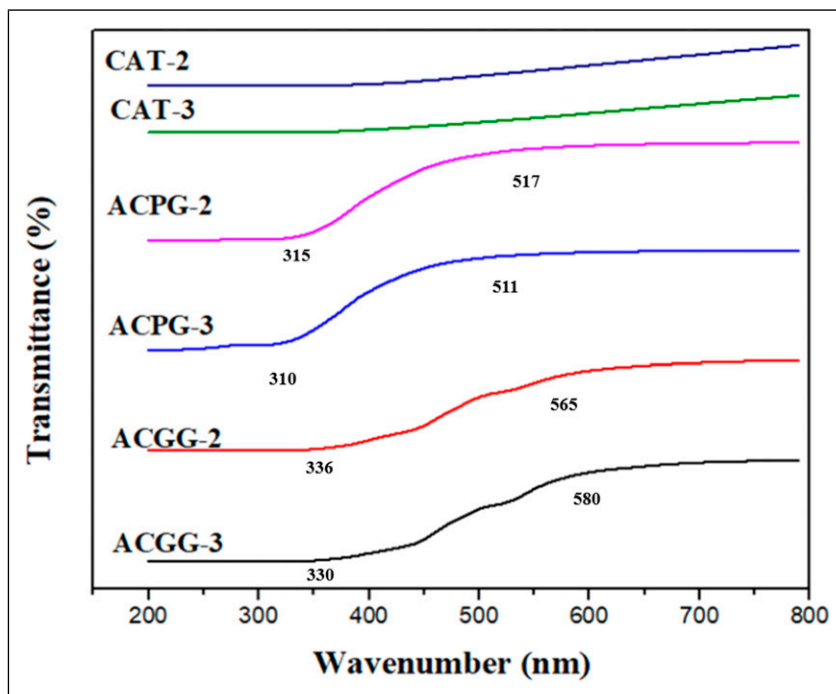


**Figure 3.** UV-Visible analysis of ACGG 2-3, ACPG 2-3, and CAT 2-3 samples.

more AV contents is shifted towards a higher wavelength. Certain active constituents in AV are responsible for absorbance in the UV region.<sup>39</sup> The absorbance peaks for ACGG-3 and ACGG-2 are observed at 336–565 nm and 330–580 nm. The sinapate esters and flavonoid compounds present in AV

gel assist in UV absorption. Furthermore, glucosamine and N-acetylglucosamine units in CS act as chromophore groups that help in UV absorption.<sup>40</sup> The spectra of ACCG-3, ACCG-2, ACPG-3, ACPG-2, CAT-3, and CAT-2 point out 90, 82, 89, 88, 37, and 34 (%) transmittance, respectively. Consequently,

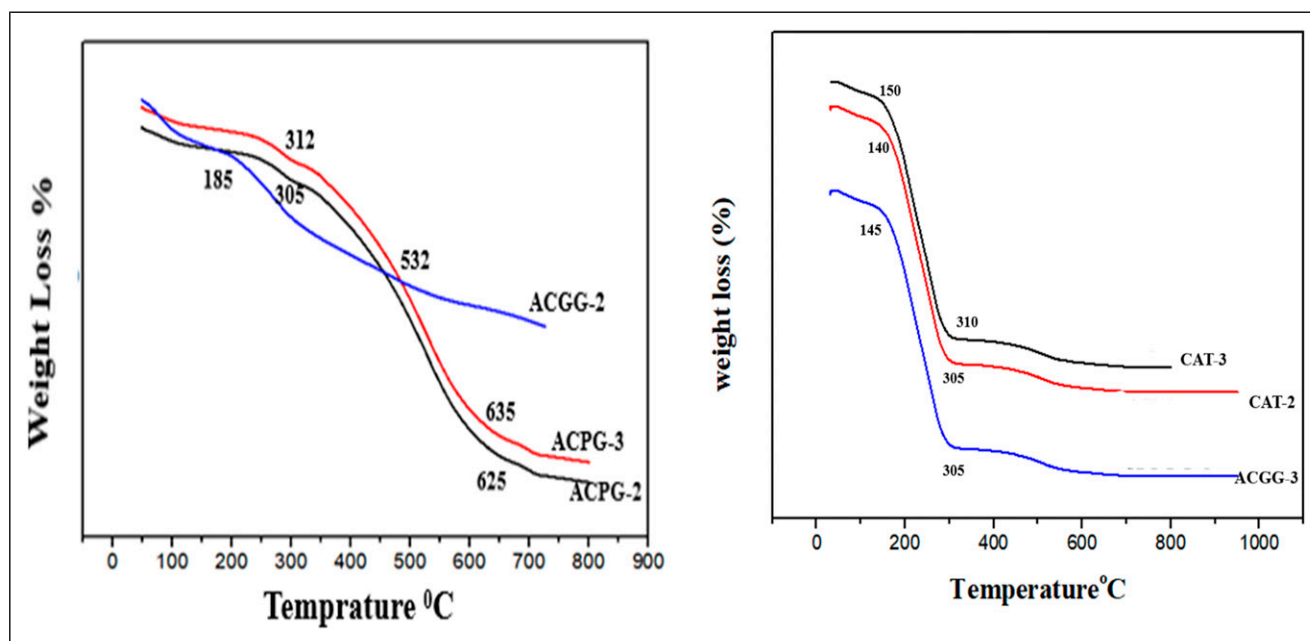


**Figure 4.** (a) TGA of ACPG-2, ACPG-3, ACGG-2 samples and (b) TGA of ACGG-3, CAT-2, and CAT-3 samples.

AV addition in membranes may provide good protection against UV-light for wound therapy.<sup>41</sup>

### Thermal Analysis

Thermal stabilization and polymeric properties have been assessed by thermogravimetry.<sup>42</sup> TGA profile of fabricated membranes displayed mass reduction in four phases (Figure 4). The first phase (71–124°C) and second phase (250–308°C) correspond to glycerine volatilization and H<sub>2</sub>O evaporation of physically and H-bonded water with chitosan.<sup>43,44</sup> Polysaccharides possess high H<sub>2</sub>O affinities and perhaps, they show disordered structural arrangements in solid states, so such macromolecules are possibly hydrated with ease. Polysaccharide's water interaction is dependent upon the basic and molecular structure, and bounded water also exerts a strong impact on the nature of polymorphic macromolecule. The bound H<sub>2</sub>O evaporation causes molecular and chemical changes during the de-acetylation process.<sup>45</sup> The third phase (312–635 C) corresponds to decomposition of branched and linear glucose chains, N-acetyl glucosamine, acetyl glucosamine units, and AV multicomponent (enzymes, minerals, anthraquinones, vitamins, fatty acid, sugars, and hormones) decomposition.<sup>13,46</sup> The fourth phase (668–725 C) designates to pyranose ring destruction and residual carbon decomposition.<sup>43</sup>

The temperature between 523 and 723 C was attributed to the total mass reduction of ammonia, water, carbon dioxide, carbon monoxide, methane, and acetic acid. The -NH<sub>2</sub> group on glucosamine unit could be released by 2 ways, that is, release of NH<sub>3</sub> and formation of hetero-aromatic ring that

confirm the bio-polymeric degradation through C-O-C bond breakage.<sup>43</sup> The CS, AV membranes demonstrated more thermal stability than CS membranes. These conclusions proposed that thermal stability of CS membranes is possibly enhanced by AV addition due to formation of glycosidic bonding as indicated in the FT-IR spectrum.

### Surface Morphology and Elemental Composition

The microstructural analysis revealed its influence on cell adhesion, migration, rapid tissue growth, and its proper functioning during wound remedy.<sup>36</sup> The SEM images of CS cross-linked membrane demonstrated smooth morphology which revealed good blending between individual constituents of the membrane (Figure 5). The SEM image of AV gel showed an interlinked channel network structure. By the addition of AV gel in CS membrane, agglomerates formation takes place. It displayed porous and rough morphology for CS, AV-gel blended membrane. The porous architecture was also noticed for CS, AV, and PVA films.<sup>36</sup> The enhanced porosity and roughness have been observed for AV, CS membranes cross-linked by genipen.<sup>47</sup> Similar findings had been indicated by Silva, proposing that the existence of AV-gel could encourage macromolecular rearrangement within the blended network, which is expressed as changes in membrane roughness.<sup>24</sup> The increased porosity influences certain features like mechanical potencies and H<sub>2</sub>O retention capabilities. Thus, the CS, AV blended membranes can easily absorb exudates and facilitate cell adherence, proliferation, and migration in porous architecture. AV gel has been claimed to possess many nutritionally important and biologically active

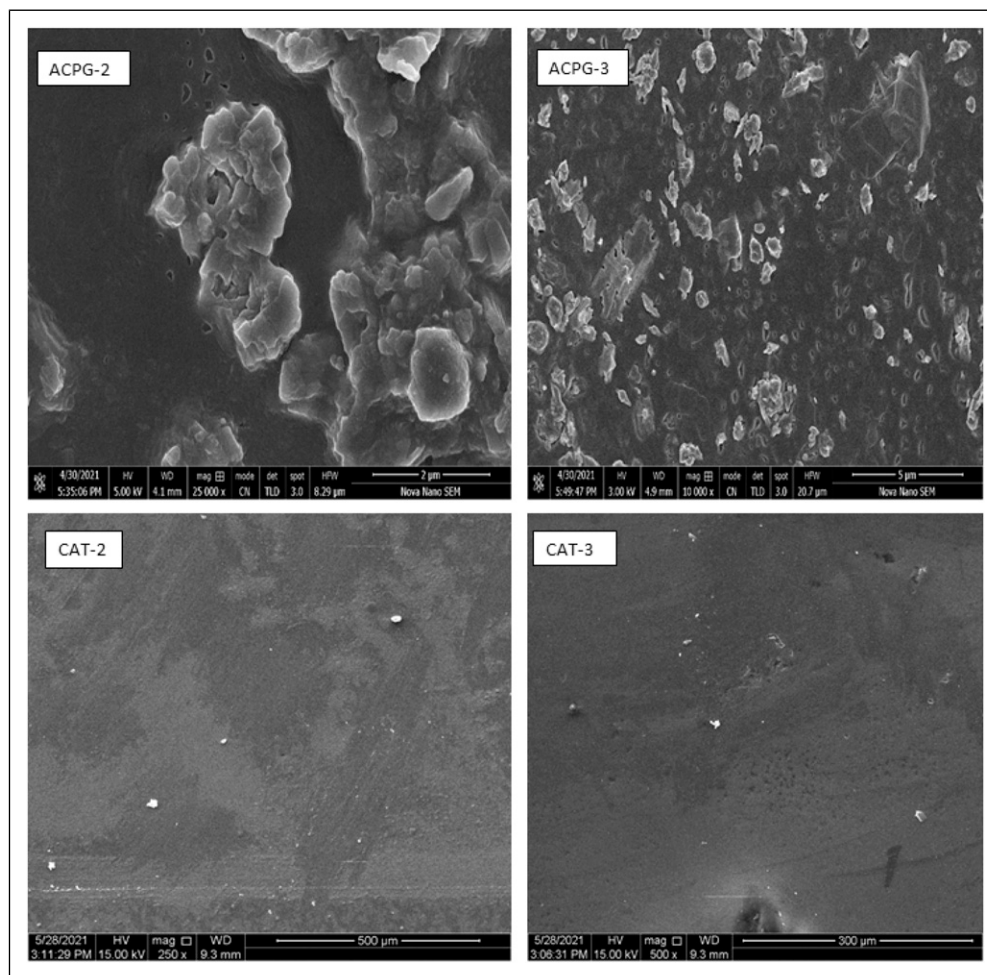


**Figure 5.** Representative SEM micrographs of AV-gel-based membranes showing their morphology.

substances like glycoproteins, vitamins, saccharides, antioxidants, and owing to their water solubility, such substances show cell attraction and promote their potential for skin lesion therapy.

### Structural Analysis

The XRD pattern (Figure 6) described the crystallinity or amorphous form of blended coating membranes because such physical nature affects polymeric properties like H<sub>2</sub>O absorption and biodegradation.<sup>48</sup> CAT membranes show 2θ values at 33.31° for CS,<sup>38</sup> 36° for CS,<sup>49</sup> 39° for AV,<sup>46</sup> and 62.61° for CS. XRD profile of CAT films displayed a slight displacement in 2θ values which indicated development of new bonds between C = O of AV and →NH<sub>2</sub> of CS, consequently confirming the bonding between CS, AV, and TW.<sup>24</sup> The diffractogram suggested amorphous nature for CAT-2 and CAT-3. The diffractive index of ACPG membranes indicated 2θ values at 36° for CS, 44.52°, 65° for AV, 38.36° for PVA.<sup>50</sup> The diffractogram of ACPG-2 and ACPG-3 shows a trivial shifting of peaks that specified the formation of new bonds

between →OH of PVA, C = O of AV, and -NH<sub>2</sub> of CS to exhibit successful bonding of individual constituents of blended membrane.<sup>36</sup> XRD analysis of ACPG-2 and ACPG-3 indicated that the increase of amorphous region and crystalline region was partially developed with well extensive chain formation. The diffractive index of ACPG-2 pointed out 2θ values at 33.31° for CS and 36° for CS.<sup>49,51</sup> The XRD of ACPG-2 pointed out the synthesis of blend based on AV, CS, GG, and glutaraldehyde by showing the existence of ester linkage between →NH<sub>2</sub> of CS and →OH of GG with glutaraldehyde.<sup>35</sup> In ACPG-2, decrease in peak lengths depicted more disarray of chain alignment after crosslinking with glutaraldehyde and exhibited amorphous structure. ACPG-3 membrane displayed 2θ values at 28.66° for CS, 47° for AV, 56.27° for AV,<sup>46</sup> 33.14° for CS,<sup>38</sup> and 70° for GG.<sup>52</sup> Therefore, the diffraction peaks are increased by PVA crosslinking, which changes intramolecular hydrogen bonding to intermolecular hydrogen bonding. The diffractogram of ACPG-2 and ACPG-3 shows a trivial shifting of peaks that specified the formation of new bonds between -OH of PVA, C = O of AV, and -NH<sub>2</sub> of CS to exhibit successful bonding of individual constituent of

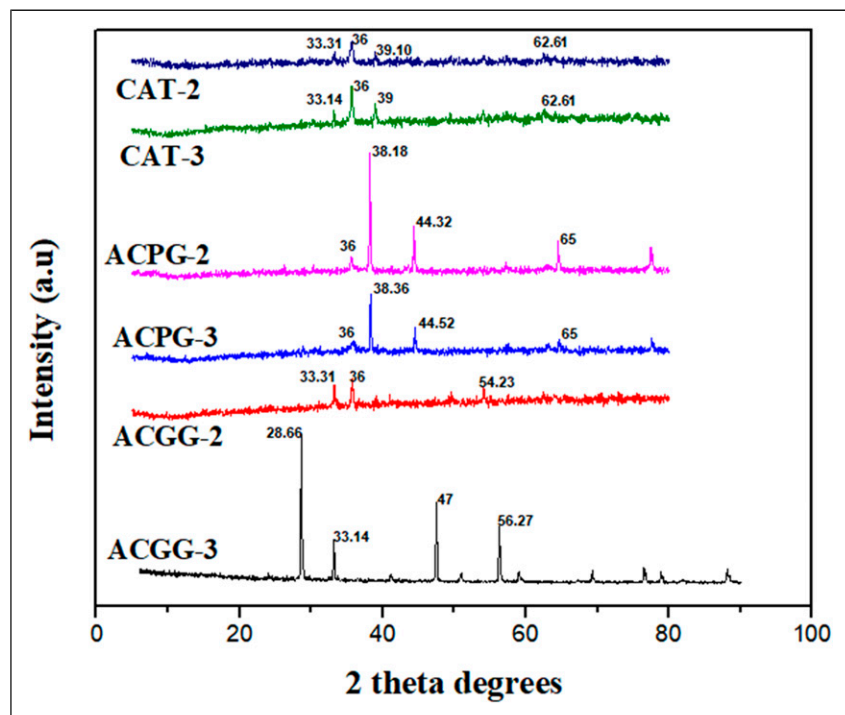


**Figure 6.** (a) XRD patterns of ACGG2, CAT-3, and CAT-2 membranes (b) ACGG-3, ACPG-3, and ACPG-2 samples.

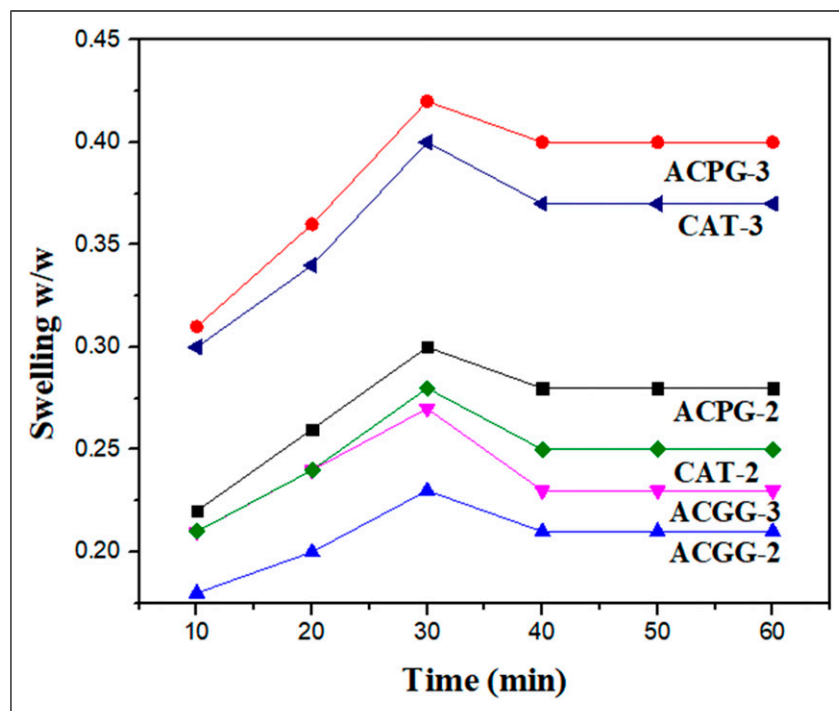


**Figure 7.** Swelling pattern of AV-gel-based membranes in aqueous medium.

blended membrane.<sup>36</sup> The overlapped patterns are found because cross-linked PVA is more crystalline than non-cross-linked and is showing larger peak area.<sup>53</sup> The graph indicated blending between AV, CS, GG, and glutaraldehyde by

representing a minimal shift in  $2\theta$  values. The presence of more AV contents in ACGG-3 created more compactness to cause more favorable H-bonding and consequently increasing crystallinity.

**Table 2.** Antibacterial Activity of AV-Gel-Based Membranes Against Gram-Positive and Gram-Negative Bacteria.

S. No	Samples	<i>E.coli</i>	<i>S.aureus</i>	<i>B.subtilis</i>	<i>P.multocida</i>
1	CAT-2	6.1 ± 0.3	7.3 ± 0.4	6.3 ± 0.9	6.2 ± 0.7
2	CAT-3	6.3 ± 0.5	7.8 ± 0.4	6.9 ± 0.7	6.6 ± 0.6
3	ACGG-2	6.4 ± 0.5	6.2 ± 0.7	6.6 ± 0.5	6.5 ± 0.8
4	ACGG-3	7.9 ± 0.7	8.4 ± 0.9	8.5 ± 0.8	7.4 ± 0.6
5	ACPG-2	8.4 ± 0.4	7.9 ± 1.3	8.5 ± 0.3	8.3 ± 0.9
6	ACPG-3	10.8 ± 1.4	9.7 ± 1.8	10.4 ± 0.9	11.6 ± 0.6
7	Norfloracin (10 µg) CT0434 B	18.5 ± 0.8	18.5 ± 0.8	18.5 ± 0.8	18.5 ± 0.8

Bacterial name: *E. coli*: *Escherichia coli*; *S. aureus*: *Staphylococcus aureus*; *B. subtilis*: *Bacillus subtilis*, and *P. multocida*: *P. multocida*. The values are mean ± SD of triplicate samples (n = 3); the standard drug norfloracin-10 µg CT0434 B) is used as control.

### Swelling Behavior of the Membranes

Swelling is the basic feature of a hydrogel. Swelling features of natural materials rely upon medium nature and diffusion of solvent in the material from an extra-cellular medium. The ACPG-2, ACPG-3, ACGG-2, ACGG-3, CAT-2, and CAT-3 membranes attained the saturation level of 329, 366, 156, 238, 211, and 344 (%), respectively, during 30 min (Figure 7). Likewise, the swelling (%) increased progressively with the increase of AV contents from 10 to 40%. The hydrophilic nature of AV polysaccharides in CS membranes might be responsible for such behavior. At swelling equilibrium, the membranes containing more than 30% AV gel resulted in a loss of structural integrity and shape due to the extremely hydrophilic behavior of AV-gel. This may cause the weakening of intermolecular interactions of CS, AV, and cross-linkers.<sup>54</sup> Based on such findings, the optimum AV gel content in the blended membrane was fixed as 30% w/v. The ACPG-3 sample with less CS concentration and more AV amount demonstrated the best swelling potential amongst others. The membranes with less CS contents and higher AV-gel amount became more porous and hold more solvent. So, this membrane reflects better swelling.

The swelling ratios of blended membranes were also observed in different pH of phosphate buffers. The swelling behavior of blended membranes was changed in different pH media due to protonation and deprotonation of functional groups. All the formulated membranes have free amino groups, polysaccharides units, and hydroxyl groups. The amino groups show attraction for protons. The concentration of protons is increased in acidic media, so the blended membranes display more swelling.<sup>55</sup> The availability of protons is less in neutral media, so the swelling behavior was decreased. Minimal H<sub>2</sub>O absorption was noticed for membranes in basic media due to decrease in protonation degree for amino groups.<sup>56</sup> Consequently, the best swelling was observed at skin pH. Increased H<sub>2</sub>O holding capability of fabricated membranes is a favorable aspect for cell attachment and growth. Similarly, the H<sub>2</sub>O holding character could facilitate nutrient transport from

membrane to cell. During wound-healing application, such membranes could prevent loss of fluids from the body at wound site.<sup>54</sup>

### Antimicrobial Activity

The antimicrobial activity was tested using disk diffusion method. Antibacterial activity of AV inclusion in chitosan was measured in terms of inhibition zone (mm) against *E. coli*, *S. aureus*, *B. subtilis*, and *P. multocida* strains and presented in Table 2. The following samples with different sample codes were selected for antibacterial screening, (CAT-2 and CAT-3, ACGG-2 and ACGG-3, ACPG-2 and ACPG-3), and 5 mm of polymeric membranes were prepared for disk diffusion assay. If we compare the CAT-2 and CAT-3, they did not show any significant antibacterial activity against panel of microorganism strain, but if we compare these concentrations among all tested microorganisms, they relatively show better activity against *S. aureus* when compared to tested strain. ACGG-2 and ACGG-3 also show a similar effect against tested bacterial strain, but among tested strain, it relatively shows better bacteriocidal against *B. subtilis*. Due to high concentration of chitosan, bioactive compounds were trapped and could not easily cross the membrane and that's why we were unable to record any significant bactericidal potential of AV inclusion in chitosan. But ACPG-2 and ACPG-3 show better antibacterial potential when compared to other samples. The antimicrobial activity profile revealed that the prepared membrane is highly active against Gram-positive and Gram-negative microbes and has potential application in biomedical field.<sup>57-65</sup>

### Conclusions

In the present study, different cross-linkers were used to prepare the aloe vera (AV) and chitosan (CS) membranes. These membranes were characterized using XRD, SEM, FT-IR spectroscopy, TGA, UV-Visible, swelling ratio, and antimicrobial studies. The membrane properties were significantly

affected by the addition of aloe vera. The ACPG-3 was found better among all prepared membranes with respect to absorption, swelling, and stability. The AV gel contents addition has really improved the surface structural properties. The antimicrobial activity was tested against *Es coli*, *S. aureus*, *B subtilis*, and *P multocida* strains and membranes showed promising antimicrobial activity. Based on these data, the prepared membranes have potential applications in the biomedical field.

### Acknowledgments

The authors extend their appreciation to Princess Nourah bint Abdulrahman University Researchers Supporting Project number (PNURSP2023R165), Princess Nourah bint Abdulrahman University, Riyadh, Saudi Arabia.

### Declaration of Conflicting Interests

The author(s) declared no potential conflicts of interest with respect to the research, authorship, and/or publication of this article.

### Funding

The author(s) disclosed receipt of the following financial support for the research, authorship, and/or publication of this article: This research was funded by Princess Nourah bint Abdulrahman University Researchers Supporting Project number (PNURSP2023R165), Princess Nourah bint Abdulrahman University, Riyadh, Saudi Arabia.

### ORCID iDs

Arif Nazir  <https://orcid.org/0000-0002-9412-6100>

Samar Z. Alshawwa  <https://orcid.org/0000-0001-9232-7956>

Munawar Iqbal  <https://orcid.org/0000-0001-7393-8065>

### References

1. Qu J, Li J, Zhu W, et al. Hybrid nanocomposite multinet network hydrogel containing magnesium hydroxide nanoparticles with enhanced antibacterial activity for wound dressing applications. *Polymer*. 2022;251:124902.
2. Yang X, Wang B, Sha D, et al. Injectable and antibacterial  $\epsilon$ -poly(L-lysine)-modified poly(vinyl alcohol)/chitosan/AgNPs hydrogels as wound healing dressings. *Polymer*. 2021;212:123155.
3. Liu C, Fu L, Jiang T, Liang Y, Wei Y. High-strength and self-healable poly (acrylic acid)/chitosan hydrogel with organic-inorganic hydrogen bonding networks. *Polymer*. 2021;230:124006.
4. Pawar HV, Tetteh J, Boateng JS. Preparation, optimisation and characterisation of novel wound healing film dressings loaded with streptomycin and diclofenac. *Colloids Surf B Biointerfaces*. 2013;102:102-110.
5. Boateng JS, Matthews KH, Stevens HNE, Eccleston GM. Wound healing dressings and drug delivery systems: a review. *J Pharm Sci*. 2008;97(8):2892-2923.
6. Gómez Chabala LF, Cuartas CEE, López MEL. Release behavior and antibacterial activity of chitosan/alginate blends with aloe vera and silver nanoparticles. *Mar Drugs*. 2017;15(10):328.
7. Gramatica P, Monti D, Speranza G, Manitto P. Aloe revisited the structure of aloeresin A. *Tetrahedron Lett*. 1982;23(23):2423-2424.
8. Atherton P. Aloe vera revisited. *Br J Phytother*. 1997;4:176-183.
9. Shelton RM. Aloe vera: its chemical and therapeutic properties. *Int J Dermatol*. 1991;30(10):679-683.
10. Atherton P. *The essential aloe vera: The actions and the evidence*. United States: Mill Enterprises; 1997.
11. Ro JY, Lee BC, Kim JY, et al. Inhibitory mechanism of aloe single component (Alprogen) on mediator release in guinea pig lung mast cells activated with specific antigen-antibody reactions. *J Pharmacol Exp Ther*. 2000;292(1):114-121.
12. Hutter JA, Salman M, Stavinoha WB, et al. Antiinflammatory C-glucosyl chromone from aloe barbadensis. *J Nat Prod*. 1996;59(5):541-543.
13. Surjushe A, Vasani R, Saple DG. Aloe vera: a short review. *Indian J Dermatol*. 2008;53(4):163-166.
14. Yebpella GG, Adeyemi HMM, Hammuel C, Magomya AM, Agbaji AS, Okonkwo EM. Phytochemical screening and comparative study of antimicrobial activity of Aloe vera various extracts. *Afr J Microbiol Res*. 2011;5(10):1182-1187.
15. Misir J, H Brishti F, M Hoque M. <i>Aloe vera</i> gel as a novel edible coating for fresh fruits: A review. *Adv J Food Sci Technol*. 2014;2(3):93-97.
16. Sánchez M, González-Burgos E, Iglesias I, Gómez-Serranillos MP. Pharmacological update properties of aloe vera and its major active constituents. *Molecules*. 2020;25(6):1324.
17. Ahmad M, Manzoor K, Singh S, Ikram S. Chitosan centered bionanocomposites for medical specialty and curative applications: A review. *Int J Pharm*. 2017;529(1-2):200-217.
18. Anitha A, Sowmya S, Kumar PS, et al. Chitin and chitosan in selected biomedical applications. *Prog Polym Sci*. 2014;39(9):1644-1667.
19. Zhang X, Yang D, Nie J. Chitosan/polyethylene glycol diacrylate films as potential wound dressing material. *Int J Biol Macromol*. 2008;43(5):456-462.
20. Sionkowska A. Current research on the blends of natural and synthetic polymers as new biomaterials: Review. *Prog Polym Sci*. 2011;36(9):1254-1276.
21. Gaaz TS, Sulong AB, Akhtar MN, Kadhum AAH, Mohamad AB, Al-Amiery AA. Properties and applications of polyvinyl alcohol, halloysite nanotubes and their nanocomposites. *Molecules*. 2015;20(12):22833-22847.
22. Rodrigues IR, de Camargo Forte MM, Azambuja DS, Castagno KR. Synthesis and characterization of hybrid polymeric networks (HPN) based on polyvinyl alcohol/chitosan. *React Funct Polym*. 2007;67(8):708-715.
23. Moeini A, Pedram P, Makvandi P, Malinconico M, Gomez d' Ayala G. Wound healing and antimicrobial effect of active secondary metabolites in chitosan-based wound dressings: a review. *Carbohydr Polym*. 2020;233:115839.

24. Silva SS, Popa EG, Gomes ME, et al. An investigation of the potential application of chitosan/aloë-based membranes for regenerative medicine. *Acta Biomater.* 2013;9(6):6790-6797.
25. Ahlawat KS, Khatkar BS. Processing, food applications and safety of aloë vera products: a review. *J Food Sci Technol.* 2011;48(5):525-533.
26. Sullad AG, Manjeshwar LS, Aminabhavi TM. Novel pH-sensitive hydrogels prepared from the blends of poly (vinyl alcohol) with acrylic acid-graft-guar gum matrixes for isoniazid delivery. *Ind Eng Chem Res.* 2010;49(16):7323-7329.
27. Riaz M, Rasool N, Bukhari IH, et al. In vitro antimicrobial, antioxidant, cytotoxicity and GC-MS analysis of Mazus goodenifolius. *Molecules.* 2012;17(12):14275-14287.
28. Chithra P, Sajithlal GB, Chandrakasan G. Influence of aloë vera on collagen characteristics in healing dermal wounds in rats. *Mol Cell Biochem.* 1998;181(1):71-76.
29. Hegggers JP, Kucukcelebi A, Listengarten D, et al. Beneficial effect of Aloë on wound healing in an excisional wound model. *J Altern Complement Med.* 1996;2(2):271-277.
30. Chithra P, Sajithlal GB, Chandrakasan G. Influence of Aloë vera on the glycosaminoglycans in the matrix of healing dermal wounds in rats. *J Ethnopharmacol.* 1998;59(3):179-186.
31. Madhumathi K, Sudheesh Kumar PT, Abhilash S, et al. Development of novel chitin/nanosilver composite scaffolds for wound dressing applications. *J Mater Sci Mater Med.* 2010;21(2):807-813.
32. Iqbal DN, Tariq M, Khan SM, et al. Synthesis and characterization of chitosan and guar gum based ternary blends with polyvinyl alcohol. *Int J Biol Macromol.* 2020;143:546-554.
33. Silva SS, Goodfellow BJ, Benesch J, Rocha J, Mano J, Reis R. Morphology and miscibility of chitosan/soy protein blended membranes. *Carbohydr Polym.* 2007;70(1):25-31.
34. Hamman JH. Composition and applications of aloë vera leaf gel. *Molecules.* 2008;13(8):1599-1616.
35. Sami AJ, Khalid M, Jamil T, et al. Formulation of novel chitosan guar gum based hydrogels for sustained drug release of paracetamol. *Int J Biol Macromol.* 2018;108:324-332.
36. Escobar-Sierra DM, Perea-Mesa YP. Manufacturing and evaluation of Chitosan, PVA and Aloë Vera hydrogels for skin applications. *Dyna.* 2017;84(203):134-142.
37. Pereira R, Carvalho A, Vaz DC, Gil MH, Mendes A, Bártolo P. Development of novel alginate based hydrogel films for wound healing applications. *Int J Biol Macromol.* 2013;52:221-230.
38. Rokhati N, Susanto H, Haryani K, Pramudono B. Enhanced enzymatic hydrolysis of chitosan by surfactant addition. *Period Polytech-Chem Eng.* 2017;62(3):286-291.
39. Subramani K, Kolathupalayam Shanmugam B, Rangaraj S, Palanisamy M, Periasamy P, Venkatachalam R. Screening the UV-blocking and antimicrobial properties of herbal nanoparticles prepared from aloë vera leaves for textile applications. *IET Nanobiotechnol.* 2018;12(4):459-465.
40. Mondal MIH, Saha J. Antimicrobial, UV resistant and thermal comfort properties of chitosan- and aloë vera-modified cotton woven fabric. *J Polym Environ.* 2019;27(2):405-420.
41. Andonegui San Martín M, Irastorza A, Izeta Permisán A, De la Caba Ciriza MC, Guerrero Manso PM. *Physicochemical and biological performance of aloë vera-incorporated native collagen films.* *Pharmaceutics;* 2020;12, 1173.
42. Fiedler JO, Carmona ÓG, Carmona CG, et al. *Application of aloë vera microcapsules in cotton nonwovens to obtain biofunctional textiles.* *The Journal of the Textile Institute;* 2019;111, 68-74.
43. Moussout H, Ahlafi H, Aazza M, Bourakhouadar M. Kinetics and mechanism of the thermal degradation of biopolymers chitin and chitosan using thermogravimetric analysis. *Polym Degrad Stabil.* 2016;130:1-9.
44. Yong H, Wang X, Bai R, Miao Z, Zhang X, Liu J. Development of antioxidant and intelligent pH-sensing packaging films by incorporating purple-fleshed sweet potato extract into chitosan matrix. *Food Hydrocolloids.* 2019;90:216-224.
45. Jang MK, Kong BG, Jeong YI, Lee CH, Nah JW. Physicochemical characterization of  $\alpha$ -chitin,  $\beta$ -chitin, and  $\gamma$ -chitin separated from natural resources. *J Polym Sci Polym Chem.* 2004;42(14):3423-3432.
46. Abdel-Mohsen AM, Abdel-Rahman RM, Kubena I, et al. Chitosan-glucan complex hollow fibers reinforced collagen wound dressing embedded with aloë vera. Part I: Preparation and characterization. *Carbohydr Polym.* 2020;230:115708.
47. Silva SS, Caridade SG, Mano JF, Reis RL. Effect of crosslinking in chitosan/aloë vera-based membranes for biomedical applications. *Carbohydr Polym.* 2013;98(1):581-588.
48. Mishra SK, Kannan S. Development, mechanical evaluation and surface characteristics of chitosan/polyvinyl alcohol based polymer composite coatings on titanium metal. *J Mech Behav Biomed Mater.* 2014;40:314-324.
49. Correa-Pacheco ZN, Bautista-Baños S, Ramos-García ML, Martínez-González MC, Hernández-Romano J. Physicochemical characterization and antimicrobial activity of edible propolis-chitosan nanoparticle films. *Prog Org Coating.* 2019;137:105326.
50. Abdeen Z, Mohammad S, Mahmoud M. Adsorption of Mn (II) ion on polyvinyl alcohol/chitosan dry blending from aqueous solution. *Environ Nanotechnol Monit Manag.* 2015;3:1-9.
51. Singh V, Tiwari A, Tripathi DN, Sanghi R. Grafting of polyacrylonitrile onto guar gum under microwave irradiation. *J Appl Polym Sci.* 2004;92(3):1569-1575.
52. Mudgil D, Barak S, Khatkar BS. X-ray diffraction, IR spectroscopy and thermal characterization of partially hydrolyzed guar gum. *Int J Biol Macromol.* 2012;50(4):1035-1039.
53. Kenawy E-RS, Kamoun EA, Ghaly ZS, Shokr A-bM, El-Meligy MA, Mahmoud YA-G. Novel physically cross-linked curcumin-loaded PVA/Aloë vera hydrogel membranes for acceleration of topical wound healing: In vitro and in vivo experiments. *Arab J Sci Eng.* 2022;48:497-514.
54. Jithendra P, Rajam AM, Kalaivani T, Mandal AB, Rose C. Preparation and characterization of aloë vera blended collagen-chitosan composite scaffold for tissue engineering applications. *ACS Appl Mater Interfaces.* 2013;5(15):7291-7298.
55. Chandrika KP, Singh A, Rathore A, Kumar A. Novel cross linked guar gum-g-poly (acrylate) porous superabsorbent hydrogels: characterization and swelling behaviour in different environments. *Carbohydr Polym.* 2016;149:175-185.

56. Wu Y-B, Yu S-H, Mi F-L, et al. Preparation and characterization on mechanical and antibacterial properties of chitosan/cellulose blends. *Carbohydr Polym.* 2004;57(4):435-440.
57. Nazir A, ur Rehman S, Abbas M, Iqbal DN, Ahsraf AR, Iqbal M. Green synthesis and characterization of copper nanoparticles using *Parthenium hysterophorus* extract: Antibacterial and antioxidant activities evaluation. *Chem Int.* 2022; 8(2):68-76.
58. George M, Ajeesha T, Manikandan A, et al. Evaluation of Cu-MgFe<sub>2</sub>O<sub>4</sub> spinel nanoparticles for photocatalytic and antimicrobial activities. *J Phys Chem Solids.* 2021;153:110010.
59. Iqbal M, Abbas M, Nisar J, Nazir A, Qamar A. Bioassays based on higher plants as excellent dosimeters for ecotoxicity monitoring: A review. *Chem Int.* 2019;5(1):1-80.
60. Almessiere M, Slimani Y, Auwal I, et al. Biosynthesis effect of *Moringa oleifera* leaf extract on structural and magnetic properties of Zn doped Ca-Mg nano-spinel ferrites. *Arab J Chem.* 2021;14(8):103261.
61. Salem NM, Awwad AM. Green synthesis and characterization of ZnO nanoparticles using *Solanum rantonnetii* leaves aqueous extract and antifungal activity evaluation. *Chem Int.* 2022;8(1): 12-17.
62. Naseer A, Iqbal M, Ali S, Nazir A, Abbas M, Ahmad N. Green synthesis of silver nanoparticles using *Allium cepa* extract and their antimicrobial activity evaluation. *Chem Int.* 2022;8(3):89-94.
63. Mouhamad RS, Al Khafaji KA, Al-Dharob MH, Al-Abodi EE. Antifungal, antibacterial and anti-yeast activities evaluation of oxides of silver, zinc and titanium nanoparticles. *Chem Int.* 2022;8(4):159-166.
64. Almessiere MA, Slimani Y, Rehman S, Khan FA, Sertkol M, Baykal A. Green synthesis of Nd substituted Co-Ni nanospinel ferrites: a structural, magnetic, and antibacterial/anticancer investigation. *J Phys D Appl Phys.* 2021;55(5):055002.
65. Hassan SM, Arshad M. Nutra-pharmaceutical potential evaluation of *Trigonella foenum graecum* seeds extracts in different solvents. *Chem Int.* 2022;8(1):23-32.